

One-dimensional electron gas in GaAs: Periodic conductance oscillations as a function of density

U. Meirav and M. A. Kastner

*Department of Physics and Research Laboratory of Electronics,
Massachusetts Institute of Technology, Cambridge, Massachusetts 02139*

M. Heiblum and S. J. Wind

IBM Thomas J. Watson Research Center, Yorktown Heights, New York 10598

(Received 30 May 1989)

A narrow channel patterned in a novel GaAs heterostructure with tunable electron density is used to study the conductance of the electron gas in the very low-density regime where only a single one-dimensional subband is occupied. Periodic oscillations of the conductance versus density and nonlinearities in the conductance suggest the formation of a one-dimensional charge-density wave or Wigner crystal.

A one-dimensional electronic system (1DES) is expected to have exotic quantum states,¹ and has been the focus of much research,² especially since new materials and fabrication technology have made such systems experimentally accessible. In recent years several groups have realized very narrow channels in GaAs heterostructures,³ where the microscopic length scales—the Fermi wavelength and the various scattering lengths—are very large. Usually the electron density in these devices is sufficiently high that several, though not many, lateral excitation states (one-dimensional subbands) are occupied, thus rendering these only a *quasi*-1DES. By using a novel heterostructure with a tunable electron density, as well as a lateral confinement scheme that allows us to change the width of a narrow channel, we confine the electrons to a single subband, thus creating a *true* 1DES in GaAs. We find that these devices show large oscillations in conductance as a function of electron density at low temperature; furthermore, in some of the devices, these oscillations are *periodic*—similar to the behavior recently observed in narrow silicon inversion layers.⁴ Our findings support the interpretation that this periodicity results from an ordered many-body ground state of the 1DES.

The devices used for this experiment were narrow channels patterned in an inverted semiconductor-insulator-semiconductor heterostructure, whose development was reported earlier.⁵ Briefly, this structure was grown by molecular-beam epitaxy on a conductive GaAs substrate, beginning with an (undoped) $\text{Al}_x\text{Ga}_{1-x}\text{As}$ barrier layer, 100 nm thick, followed by an undoped layer of GaAs, 120 nm thick, and finally a planar doping sheet and a cap layer, 20 nm thick. In equilibrium, the undoped GaAs layer has no carriers, and is therefore insulating. However, with the application of a positive voltage to the substrate with respect to the undoped GaAs layer (the gate voltage, V_g), a two-dimensional electron gas (2DEG) forms at the lower GaAs interface. The density of this 2DEG can be controllably tuned from threshold up to about $7.0 \times 10^{11} \text{ cm}^{-2}$, where, due to the high V_g , gate leakage current through the $\text{Al}_x\text{Ga}_{1-x}\text{As}$ barrier becomes significant. The 2DEG Hall mobility at 4.2 K for densities above $3 \times 10^{11} \text{ cm}^{-2}$ was over $5 \times 10^5 \text{ cm}^2/\text{V sec}$, but it rapidly

decreased as the density was lowered. A narrow channel was defined by a gap in a *p*-type implant, a method used previously on Si accumulation layers⁶ (shown in the lower inset of Fig. 2). The gap, $1.0 \mu\text{m}$ wide, was patterned by electron beam lithography. The electronic width W is much smaller than that of the implant gap, as will be discussed shortly. Furthermore, W can be changed by applying a negative pinching voltage V_p to the implanted regions, relative to the 2DEG. Channels with lengths of $2 \mu\text{m}$ and $8 \mu\text{m}$ were made.

Devices were cooled in a dilution refrigerator and their conductance G was measured as V_g was slowly raised, using standard small signal ac lock-in techniques. Whereas the 2DEG began accumulating and conducting at $V_g \sim 0.1 \text{ V}$, the narrow channels had much higher thresholds, between $0.5\text{--}0.7 \text{ V}$, beyond which their conductance gradually increased. At relatively high temperatures ($T > 2 \text{ K}$), the conductance rose quite smoothly with V_g . However, at $T < 1 \text{ K}$, the conductance showed dramatic oscillations as V_g was increased. Figure 1(a) shows results of measurements at 50 mK. These were perfectly reproducible as long as the device remained cold. Most striking is the fact that they appear periodic in V_g , i.e., in carrier concentration. The periodicity is verified by Fourier transform of the data [Fig. 1(b)], showing a clear peak at a period of $\Delta V \approx 1.7 \text{ mV}$. Although all devices measured had similar fluctuations, only in some of them was a periodicity apparent. The value of ΔV varied between $1\text{--}2 \text{ mV}$ among different devices. Even in the ones with no clear periodicity, this was the typical spacing between peaks. Application of a negative V_p caused a small increase in the spacing between oscillations as the channel became narrower.⁶ Warming a given device to room temperature and cooling it down again changed the oscillation pattern. The oscillations typically persisted over a range of $\sim 30 \text{ mV}$ in V_g above threshold, beyond which they ceased quite abruptly. The values of the conductance in this near-threshold regime of oscillations were at least an order of magnitude smaller than the quantum value of e^2/h , typical of ballistic transport seen in short, narrow channels in GaAs.³

In order to make a quantitative interpretation of our

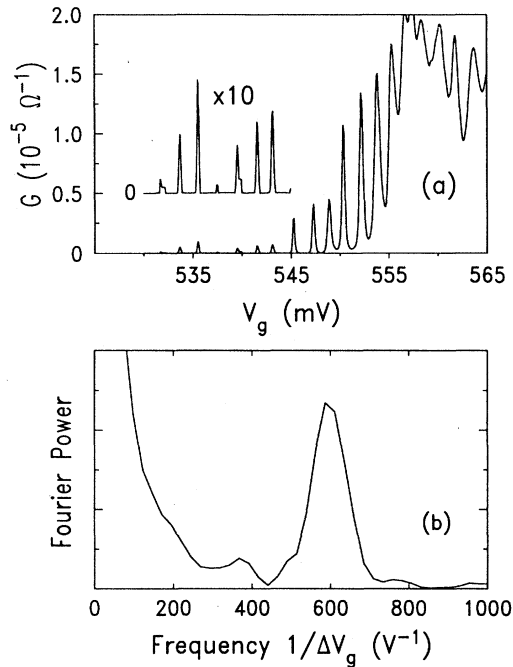


FIG. 1. (a) Conductance vs gate voltage of a narrow channel, $2 \mu\text{m}$ long, measured at $T = 50 \text{ mK}$. The inset shows an expansion of the first few oscillations. (b) Fourier power spectrum of the above. The peak corresponds to a period of $\Delta V \approx 1.7 \text{ mV}$.

data, estimates are needed of the width W , and the electron concentration N (per unit length) vs V_g . We therefore carried out computer simulations⁷ of the potential and charge distribution in our structure, solving the Poisson equation with Fermi-Dirac carrier statistics and the appropriate material parameters. The simulation did not include some factors that could affect the precise value of the threshold gate voltage, in particular, unintentional charges in the $\text{Al}_x\text{Ga}_{1-x}\text{As}$ barrier and at the interface,⁵ as well as the precise amount of charge depletion at the top surface. Still, we expect this to be a reasonable model for the dependence of N and W on small changes in V_g near threshold. Quantum corrections to the screening are not significant since we are considering *threshold* behavior, where N is very small.

We find (Fig. 2, top inset) that for V_g near threshold, the potential across the channel is almost perfectly parabolic, $V(x) = \alpha x^2$, where x is the distance from the center of the channel. The value of α depends on V_g and V_p as well as on the precise parameters used for the doping profile, about which there is some uncertainty, primarily because of dopant diffusion during annealing, but typically $\alpha \sim (1-2) \times 10^8 \text{ eV/cm}^2$. As V_g is increased and more charge accumulates in the channel, the potential becomes wider and shallower. A parabolic potential well has energy levels $E_n = (n + \frac{1}{2})\hbar\omega$ where the frequency ω is given by $\frac{1}{2}m^*\omega^2 = \alpha$, and m^* is the effective mass. Hence the subband spacing is $\Delta E = \hbar\omega \approx 1.5-2 \text{ meV}$. The ground-state wave function of such a well is a Gaussian $\psi(x) \sim \exp(-x^2/2\Lambda^2)$ with a full width at half maximum $2\Lambda = 2(\hbar/m^*\omega)^{1/2} \sim 50 \pm 5 \text{ nm}$ for our range of param-

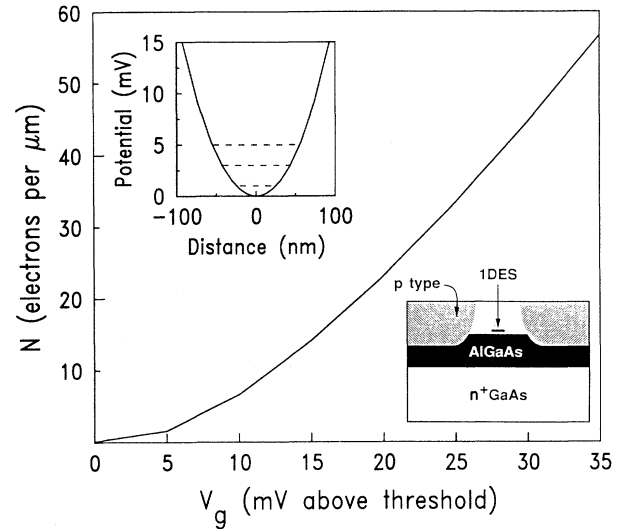


FIG. 2. Results of a computer simulation of our device, showing the density N vs V_g , where V_g is measured relative to the threshold voltage. The top inset shows the calculated potential on a cross section of the channel for V_g at threshold, with dashed lines marking the first three energy levels.

ters. This means that over 95% of the electron density, $|\psi|^2$, is confined within a width of $\sim 70 \text{ nm}$.

More important, however, is the density $N = N_c$ at which electrons begin to occupy the second subband, and the relation between N and V_g . At $T = 0$, second-subband occupation begins when the Fermi energy E_F (measured from E_0 , the lowest allowed energy state) equals $\hbar\omega$, and E_F is related to the density of a 1DES by $N = (8m^* \times E_F)^{1/2} / \hbar\pi$, giving a crossover density of $N_c = (3.6 \pm 0.3) \times 10^5 \text{ cm}^{-1}$, or ~ 36 electrons per μm . By computer simulation we also determine N vs V_g (Fig. 2), from which we can deduce that second-subband occupation begins around 25–30 mV above threshold. Actually, some correction is expected due to the lowering of α that occurs as V_g is raised; however, since $N_c \propto \alpha^{1/4}$, the correction is very small. This range of V_g is in remarkable agreement with the experimentally observed range of sharp oscillations, suggesting a correlation between the occurrence of the oscillations and the regime of single-subband occupation. From Fig. 2 we also find the capacitance of the device, in electrons per unit length per gate voltage, to be $C \sim 2 \times 10^7 \text{ cm}^{-1} \text{ V}^{-1}$, in the range corresponding to the observed oscillations. Using this approximate value, the typical spacing between oscillations yields a length scale $L_0 \equiv (\Delta VC)^{-1} \sim 0.5-1 \mu\text{m}$, corresponding to a segment of the 1DES which has *one electron* added to it between consecutive oscillations.

We now turn to the question of the mechanism leading to the observed phenomenon. Our simulations indicate that the regime of the oscillations coincides with single-subband population, i.e., a true 1DES. As first realized by Peierls,⁸ even the noninteracting 1DES is inherently unstable, forming of a charge-density wave (CDW) with a wave vector of $2k_F$ (where k_F is the Fermi wave vector), accompanied by a lattice distortion. Such a lattice distur-

tion is not expected in our devices, however, primarily because the lattice is three dimensional and extended. The *interacting* 1DES is also unstable towards forming an additional host of broken-symmetry ground states,¹ including a $2k_F$ spin-density wave (SDW) and a $4k_F$ CDW.⁹ At a sufficiently low density or strong interaction, a one-dimensional (and probably antiferromagnetic) Wigner crystal (WC) should form, which can be viewed as an extreme case of the $4k_F$ CDW. Note that $4k_F$ corresponds to the spatial periodicity of the average interelectron spacing, $1/N$.

Such a CDW would be pinned to impurities,¹⁰ and the strength of the pinning is sensitive, among other things, to the commensurability of the CDW and the distance between pinning centers. Following Scott-Thomas *et al.*,⁴ we propose the formation of a pinned WC or CDW (but, specifically, a $4k_F$ wave) as the source of the oscillations of conductance versus V_g . The oscillations arise in the following way. When a CDW is pinned at several points, the pinning strength is maximized when the spacing between the pinning centers is an integral number of periods of the density wave, namely the interelectron spacing $1/N$. This condition is referred to as commensurability. As V_g , and hence N , are increased, the pinning strength oscillates, and with it G oscillates as well, reaching a minimum (of G) each time the commensurability condition is satisfied. In order for this mechanism to cause simple *periodic* oscillations, it is necessary for the conductance to be determined by one dominant pinning segment. In fact, within this picture, each oscillation cycle corresponds to a rise in N so that *one electron* is added to such a segment, and the length of this segment is the same L_0 derived earlier from the period ΔV , namely $0.5\text{--}1\ \mu\text{m}$. The length of a pinning segment is simply the spacing between two impurities along the channel. Such an impurity spacing along a channel of this width, namely $\sim 1\ \mu\text{m}$, is in agreement with our previous estimates for the interface impurity density derived from mobility measurements.⁵ This model can explain why the oscillations are sample dependent and change when a sample is warmed and cooled again, as impurities may redistribute. Furthermore, similar but non-periodic oscillations are interpreted as a result of more than one dominant pinning segment.

One of the characteristics of a pinned CDW is the non-linearity of the conductance¹⁰ in the applied dc bias along the channel, V_{ds} . Figure 3 shows the dependence of G on V_{ds} when V_g was held fixed, both at a maximum and at a minimum of an oscillation. A steep rise in G is seen at $V_{ds} \sim \pm 0.5\ \text{mV}$, as well as complex structure in G , which is not symmetric in V_{ds} . Similar structure was seen for all minima and maxima in V_g . This behavior supports the pinned CDW picture, with the rise in G attributed to depinning by the applied electric field. It is worth pointing out that a bias along the channel creates a difference in the effective gate voltage at different points along the channel. Some of the detailed features in these scans may be related to this fact. Still, the scale of steep rise in G is much too large to be attributed only to this effect.

The mechanism of conduction at zero bias is not clear. The possibilities we considered included thermally activated depinning or quasiparticle excitations, which would re-

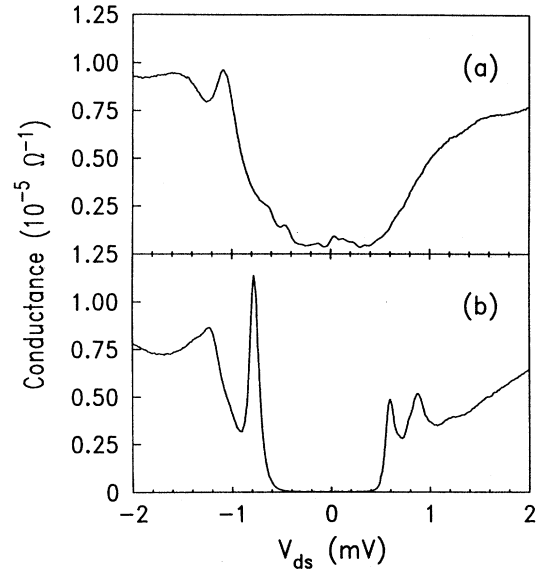


FIG. 3. Conductance vs the applied dc bias, V_{ds} . Here V_g is held fixed at (a) a maximum, and (b) a minimum, of the same oscillation.

sult in a strong dependence of G on T at low temperatures. We repeated our measurements of G vs V_g at various temperatures. Up to $\sim 0.3\ \text{K}$ we find almost no change in G . As T is further raised, the conductance rises and the oscillatory structure smears out, virtually disappearing by $T \sim 2\ \text{K}$. In Fig. 4 we show the dependence of G on T both at a minimum and a maximum. Note that, unlike the minima near threshold shown in Fig. 1, this minimum had a measurable, nonzero conductance at all temperatures. The range of T where G is strongly temperature dependent is too narrow to conclude whether G exhibits

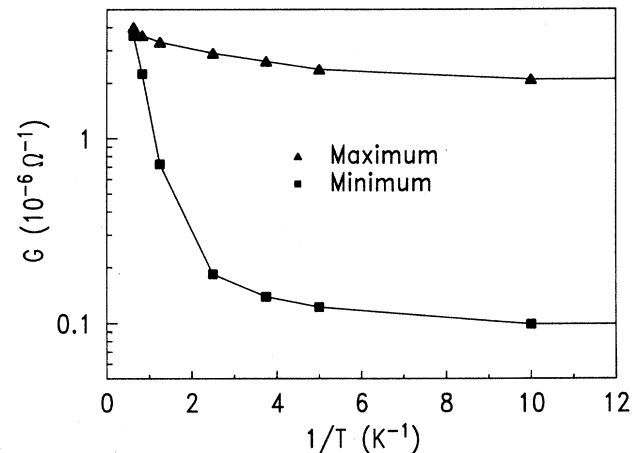


FIG. 4. Arrhenius plot showing temperature dependence of G , at a maximum and at a minimum of an oscillation. No changes were observed between 50 and 100 mK. Note that the minimum shown here had a nonzero conductance even at the lowest temperatures.

thermally activated behavior, but if it *is* thermally activated, the activation energy would be roughly 1–2 K.

The weak temperature dependence at low T is surprising in light of previous results.⁴ Careful measures were taken to eliminate possible sources of electronic heating, and it is unlikely that heating can explain our observations. Another possibility is that the low- T , low-bias conduction is dominated by tunneling, as first suggested by Bardeen¹¹ in the context of phonon-coupled CDW's. Although the Bardeen picture may not be applicable to our system, where phonons are not directly involved, and only a single, short chain of electrons exists, the possibility of tunneling is facilitated by the small effective mass in GaAs. A more promising model for our observations is the soliton tunneling picture of CDW's through impurities, proposed by Larkin and Lee.¹² We are currently studying the applicability of this picture to our system. At higher T , however, a crossover to a thermally activated

mechanism seems to occur before the system loses its ordered state.

In conclusion, a true one-dimensional electron system has been created in GaAs. The strong periodic oscillations in its conductance versus the electron density suggest that a broken-symmetry many-body ground state is formed, such as a one-dimensional Wigner crystal or charge-density wave, which is pinned to the lattice by impurities. Low-temperature conduction may be dominated by tunneling.

We would like to thank Stuart B. Field for useful discussions and experimental help, and B. I. Halperin for his suggestions. We also thank H. Shtrikman for help with the sample growth. This work was supported by National Science Foundation Grant No. ECS-8503443 and by the U.S. Joint Services Electronics Program under Contract No. DAA/03-86-K-0002.

¹J. Solyom, *Adv. Phys.* **28**, 201 (1979), and references therein.

²See, for example, *Highly Conductive One-Dimensional Solids*, edited by J. T. Devreese, R. D. Evrard, and V. E. van Doren (Plenum, New York, 1979).

³For a recent compilation of the work done in this field, see *Proceedings of the Fifth International Winter School, Mautendorf, Austria, 1988*, edited by H. Heinrich, G. Bauer, and F. Kuchar, Springer Series in Solid State Sciences, Vol. 83 (Springer-Verlag, New York, 1988).

⁴J. H. F. Scott-Thomas, Stuart B. Field, M. A. Kastner, Henry I. Smith, and D. A. Antoniadis, *Phys. Rev. Lett.* **62**, 583 (1989).

⁵U. Meirav, M. Heiblum, and Frank Stern, *Appl. Phys. Lett.* **52**, 1268 (1988).

⁶A. B. Fowler, A. Hartstein, and R. A. Webb, *Phys. Rev. Lett.* **48**, 196 (1982); C. C. Dean and M. Pepper, *J. Phys. C* **15**,

L1287 (1982); A. Ya. Shik, *Fiz. Tekh. Poluprovodn.* **19**, 1488 (1985) [*Sov. Phys. Semicond.* **19**, 915 (1985)].

⁷M. R. Pinto, C. S. Rafferty, and R. W. Dutton, computer code PISCES-II (Stanford Electronics Laboratory, Stanford University, Stanford, CA 94305).

⁸R. E. Peierls, *Quantum Theory of Solids* (Oxford, London 1955), p. 108.

⁹J. B. Torrance, in *Chemistry and Physics of One Dimensional Metals*, edited by Heimo J. Keller (Plenum, New York, 1976), p. 137–166, and references therein.

¹⁰P. A. Lee and T. M. Rice, *Phys. Rev. B* **19**, 3970 (1979), and references therein.

¹¹John Bardeen, *Phys. Rev. Lett.* **42**, 1498 (1979); *Z. Phys. B* **67**, 427 (1987).

¹²A. I. Larkin and P. A. Lee, *Phys. Rev. B* **17**, 1596 (1978).